Bull. Mater. Sci., Vol. 29, No. 3, June 2006, pp. 293–301. © Indian Academy of Sciences.

Characterization of zinc–nickel alloy electrodeposits obtained from sulphamate bath containing substituted aldehydes

VISALAKSHI RAVINDRAN* and V S MURALIDHARAN
Central Electrochemical Research Institute, Karaikudi 630 006, India

MS received 20 September 2005; revised 2 January 2006

Abstract. Zinc alloy offers superior sacrificial protection to steel as the alloy dissolves more slowly than pure zinc. The degree of protection and the rate of dissolution depend on the alloying metal and its composition. Zinc-nickel alloy may also serve as at less toxic substitute for cadmium. In this paper the physico-chemical characterization of zinc-nickel electrodeposits obtained from sulphamate bath containing substituted aldehydes was carried out using hardness testing, X-ray diffraction, and corrosion resistance measurements. The corrosion behaviour of these samples in a 3·5% NaCl solution was examined. The decrease in I_{corr} and high charge transfer resistance indicated the improved corrosion resistance of these deposits.

Keywords. Zinc–nickel electrodeposits; aldehydes; alloy characterization; surface morphology.

1. Introduction

Zinc–nickel electrodeposits have long been known. The codeposition of iron group metals with zinc or with each other exhibit anomalous behaviour, the retardation of deposition of the more noble metal by zinc (Ravindran and Muralidharan 1996). Zinc–nickel coatings offer enhanced corrosion protection to steel than cadmium (Ravindran and Muralidharan 1995). Zinc-nickel electrodeposition from various bath formulations was attempted (Rajagopalan 1972). Sulphate baths in the pH range of 1·5–2·5 and pH 4 with addition of boric acid and *p*-toluene sulphonic acid were used (Tsuda and Kurimoto 1981). Sulphate–sulphamate combinations produced a wide range of Zn–Ni deposits. Chloride baths with $SrSO_4$ gave bright deposits. To increase the nickel content to above 15%, boric acid was added to the acetate baths. Known brighteners and leveling agents are used to obtain non-pitted Zn–Ni alloy deposits. From sulphamate bath, in the absence of any additive, the deposit was found to be pitted (Ravindran and Muralidharan 2003). Grey, uniform, semi bright deposits were seen only in the presence of boric acid, sodium lauryl sulphate and *b*-napthol. To improve the appearance, substituted aldehydes were added to zinc plating baths (Shabana Begum *et al* 2001). It is of interest to study the role of substituted aldehydes in sulphamate bath on the surface morphology and corrosion resistance behaviour of Zn–Ni alloy deposits as these baths offer 98–99% current efficiency in the current density range of 0·5–2·0 A/dm^2.

*Author for correspondence (visalakshi47@yahoo.com)

2. Experimental

2.1 *Electrodeposition*

Cold rolled steel plates were degreased with trichloroethylene and alkaline electrocleaned cathodically for 2 min and anodically for 30 s in a solution of 35 g/l NaOH + 25 g/l Na_2CO_3 at 30°C. They were washed in running water and given a dip for 10 s in 5% H_2SO_4 solutions. Finally thorough washing and drying were resorted to. Electrodeposition was carried out using a d.c. source, a calibrated ammeter along with a cell. The prepared mild steel panels ($10 \times 7{\cdot}4 \times 0{\cdot}05$ cm) were used as cathodes. Electrolytic zinc and electrolytic nickel were used as anodes. Zinc sulphamate was prepared by dissolving ZnO in sulphamic acid (99% purity). Analar grade nickel sulphamate was used. Sulphamate complexes brought the deposition potentials of zinc and nickel closer and the alloy deposition was of 98–99% efficiency. Substituted aldehydes and other chemicals employed were of analar grade.

2.2 *Passivation treatment*

Zn–Ni alloy electrodeposits were subjected to chromating treatments. The CRONAK process involves the treatment of electrodeposits in 200 g/l Na_2CrO_4 with 6 ml/l of H_2SO_4. The treatment time was 30 s at 30°C.

2.3 *Electrochemical studies*

Table 1 summarizes the conditions under which the deposits were obtained. Electrochemical polarization studies

were carried out for various deposits. One sq.cm area of the deposits was exposed in a 5% NaCl solution at 30°C at 5 mV/s. A large platinum foil was used as an auxiliary and a saturated calomel electrode (SCE) as reference electrode, respectively.

2.4 *X-ray fluorescence*

The composition of the coatings were analysed for the percentage composition of zinc and nickel (within ± 1% error) by X-ray fluorescence (CMI W target).

2.5 *Hardness*

The hardness of the deposits was measured using LECO microhardness tester (M 400) on the Vicker's scale. This uses a diamond pyramid of a square base with an angle of 136° at the vertex between two opposite faces. The microhardness of the deposit in kg/mm^2 was determined in each case by using the following formula:

$$\text{Hardness (kg/mm}^2) = \frac{1854 \times p}{d^2},$$

where p is the load applied in grams and d the diagonal of the indentation (μm). 50 g load was applied.

2.6 *Surface morphology*

Preliminary studies showed that among the aldehydes studied, the presence of formaldehyde alone, anisaldehyde and furfuraldehyde in combination in the plating bath conferred some brightness to the deposits. To understand the nature of these deposits they were studied using a scanning electron microscope, JEOL (JSM-35 LF). The deposits were viewed at 25 kV with 1000× magnification. For these studies the plated panels were cut to 10 × 10 mm size and cold mounted, examined and photographed.

Table 1. Composition of various plating baths.

Deposit	Thickness (μm)	Bath	Composition
A	18	A	0·5 M zinc sulphamate 0·5 M nickel sulphamate 50 g/l boric acid 60 g/l ammonium chloride 0·3 g/l *b*-napthol 0·9 g/l sodium lauryl sulphate
B	14	B	A + 2·00 ml/l acetaldehyde
C	18	C	A + 1·25 ml/l anisaldehyde
D	30	D	A + 1·25 ml/l benzaldehyde
E	40	E	A + 0·90 ml/l formaldehyde
F	40	F	A + 1·00 ml/l furfuraldehyde
G	40	G	A + 1·00 ml/l furfuraldehyde + 2·00 ml/l anisaldehyde

Deposition conditions: 1·5 A/dm^2; 60 min stirring, 328 K, pH 3–4.

2.7 *X-ray diffraction*

X-ray diffraction studies of the alloy deposits were carried out by using a computer controlled X-ray Diffractometer JEOL (8030 model) with CuK_a (nickel-filtered) radiation at a rating of 40 kV, 20 mA. The scan rate was 0·05° per step and the measuring time was 15/step.

2.8 *Corrosion studies*

2.8a *Salt spray tests:* For salt spray tests, the edges of the deposits and other uncoated portions were masked completely with araldite resin. The panels were suspended in the salt spray cabinet (Heraus_Votsch) containing 5% NaCl solution. Spraying was done at the rate of 8 h spray and 16 h rest in the cabinet. Observations were made at the end of each day. An air pressure of 1·05 kg/cm^2 was maintained for the spray. The extent of corrosion was assessed usually at 24 h intervals by counting rusted and rust coloured areas with the aid of marked perplex sheet. Two or three specimens were subjected to the test under identical conditions.

2.8b *Impedance and polarization studies:* For electrochemical impedance and potentiodynamic polarization studies, PAR EG & G electrochemical system was used. Impedance measurements were made in the frequency range 0·1–1 KBZ.

3. Results

3.1 *X-fluorescence and hardness*

Increased nickel contents in the Zn–Ni deposits containing aldehydes contribute to increasing hardness of the deposits (table 2). The hardness value of the deposits obtained from the bath containing anisaldehyde, which has the highest nickel content of 28·3%, is 90·2 H_v. Zinc–

Table 2. XRF and hardness data of the deposits.

Deposit	Wt % zinc	Wt % nickel	Hardness (H_v)
A	85·0	15·00	75·8
B	87·1	12·90	71·2
C	71·7	28·30	90·2
D	78·9	21·10	79·2
E	82·8	17·20	58·6
F	82·3	17·70	56·3
G	73·0	21·00	99·0

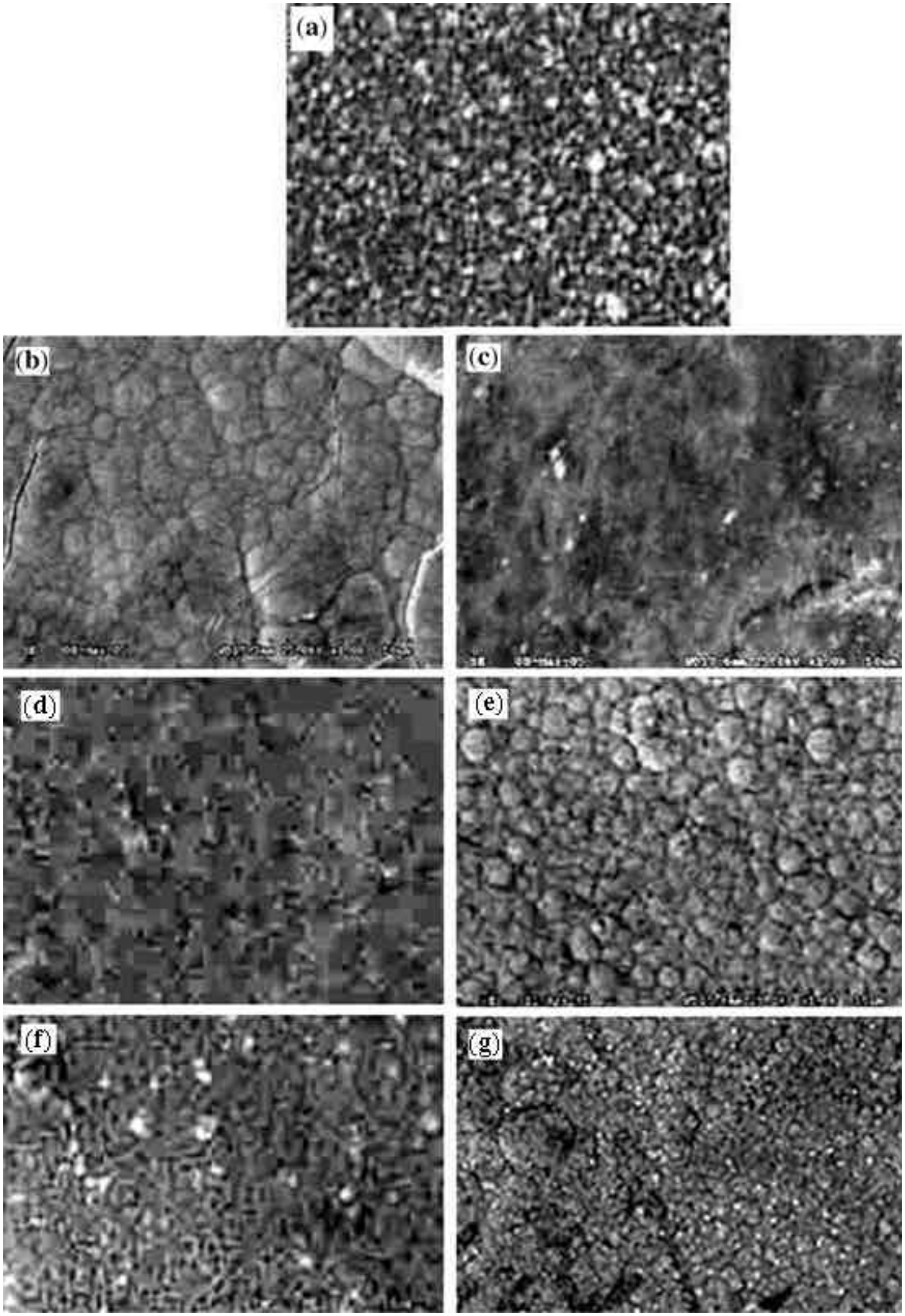

Figure 1. Scanning electron micrographs: (**a**) deposit A, (**b**) deposit E (0·12 ml/l), (**c**) deposit E (0·24 ml/l) 1·5 A/dm^2, (**d**) deposit E (0·24 ml/l) 3·0 A/dm^2, (**e**) deposit C, (**f**) deposit F and (**g**) deposit G.

nickel deposit obtained from bath containing anisaldehyde and furfuraldehyde has the highest value of 99·9 H_v.

3.2 *Scanning electron microscopy*

The zinc nickel alloy electrodeposited at a current density of 1·5 A/dm^2 was found to have an etched and non uniform surface (figure 1a). The deposit obtained from formaldehyde (0·12 ml/l) added to the bath had small crystallites covering the entire surface (figure 1b). In the presence of formaldehyde (0·24 ml/l) in the bath a semi bright, very smooth surface with small crystallites was seen (figure 1c). On raising the current density to 3 A/dm^2, bigger crystallites causing a dense coverage was observed. Hydroxide flakes were seen (figure 1d). Deposits obtained from 1·25 ml/l of anisaldehyde added bath were seen to have a smooth surface (figure 1e). Deposit with furfuraldehyde addition made the surface to have smaller tubular structures spread over the surface (figure 1f). With the combined presence of anisaldehyde and furfuraldehyde in the deposit, the surface was seen to be very smooth and semi bright (figure 1g).

3.3 *Corrosion resistance*

3.3a *Salt spray tests:* The zinc alloy deposited panels were taken out after every 24 h of test, dried and inspected visually. Table 3 summarizes the results of corrosion studies by salt spray in 5% NaCl solutions. Deposit A exhibited white rust initiation at the end of 144 h and red rust initiation at the end of 456 h. Deposit A after chromate passivation exhibited white rust at the end of 432 h and red rust at the end of 480 h. Except deposit C, all other deposits postponed white and red rust formation. Passivation had no beneficial effect on the deposits obtained in the presence of aldehydes. However, other than deposit C others offered protection against red rust formation.

Table 3. Initiation of white and red rust formation.

	Time for white rust formation (h)		Time for red rust initiation (h)	
Deposit	Passivated	Unpassivated	Passivated	Unpassivated
A	144	432	426	480
B	240	264	432	480
C	48	288	120	420
D	228	264	600	720
E	228	264	600	672
F	210	288	430	540

Table 4. Parameters derived from potentiodynamic polarization method in 3% NaCl solution.

		Tafel slope (mV/decade)		Corrosion current density (μA/cm^2)	
Deposit	E_{corr} (mV)	Anodic	Cathodic	Anodic	Cathodic
A	–981	98	96	48	48
B	–1065	40	96	6·4	7·3
C	–1010	29	28	5·2	5·0
D	–1010	49	45	3·9	3·6
E	–1051	60	190	2·3	2·0
F	–1040	53	142	3·6	3·1

Table 5. Parameters derived from impedance diagrams.

	First semi circle		Second semi circle	
Deposit	R_{ct} (ohm/cm^2)	C_{dl} (μF/cm^2)	R_{ct} (ohm/cm^2)	C_{dl} (μF/cm^2)
A	–	–	28.57	53.2
B	138·9	4·03	447·00	–
C	91·5	29	197·80	26
D	220·7	94	839·80	9
E	–	–	750·81	10
F	98·0	54·4	173·90	5·1
G	140·1	5·94	226·00	5·1

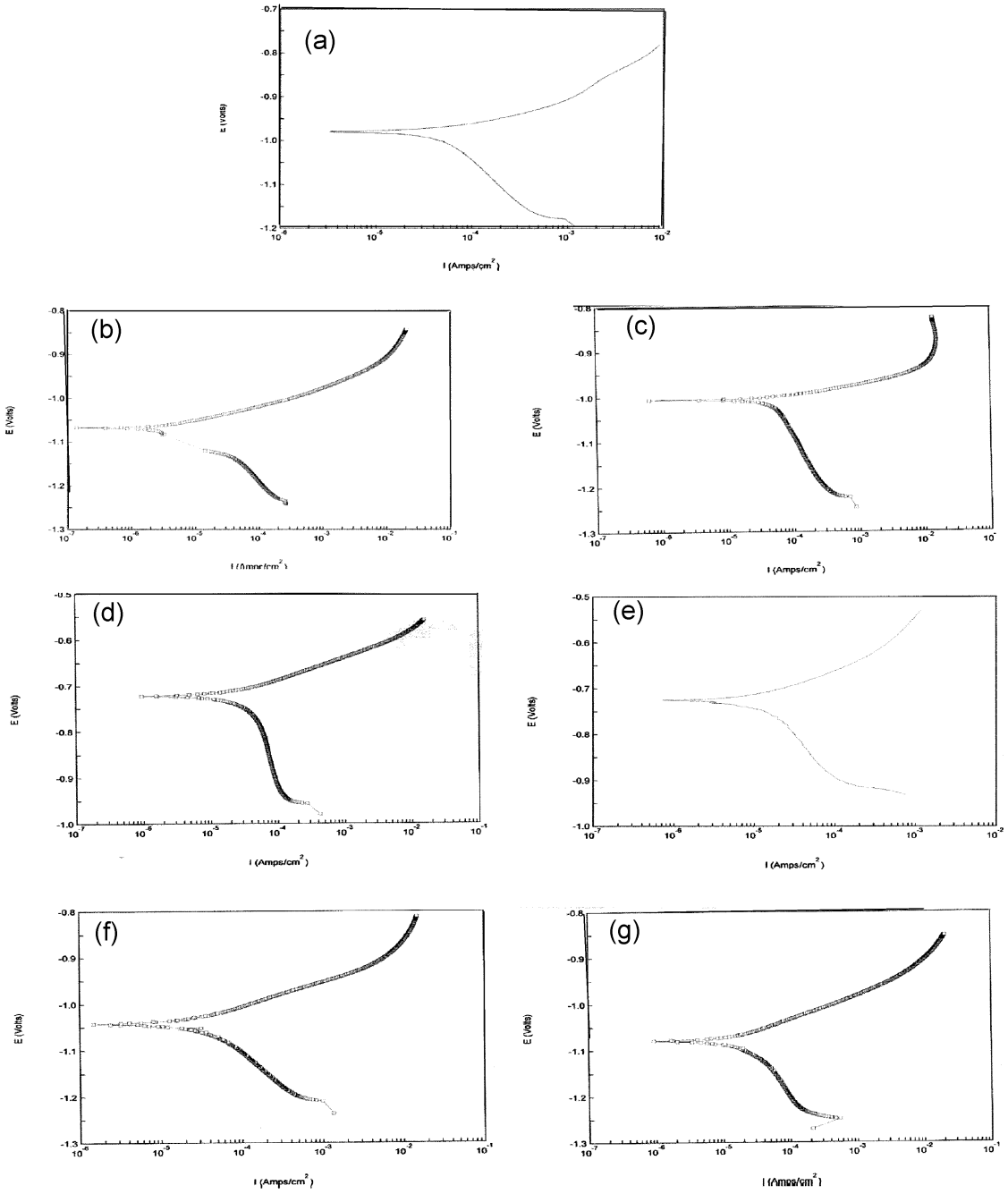

Figure 2. Polarization curves (*E*-log *i*) for the corrosion in 5% NaCl solution: (**a**) deposit A, (**b**) deposit B, (**c**) deposit C, (**d**) deposit D, (**e**) deposit E, (**f**) deposit F and (**g**) deposit G.

3.3b *Potentiodynamic polarization:* From the electrochemical theory of corrosion (Wagner and Traud 1938), corrosion current densities can be obtained by extrapolating the linear segments of anodic and cathodic (E-log i) curves. The slopes of the linear segments of anodic and cathodic branches give the anodic and cathodic tafel slopes. b_a = anodic tafel slope = RT/a_aF, b_c = cathodic tafel slope = $-RT/a_cF$, where a_a, a_c are anodic and cathodic transfer coefficients. Polarization curves for the zinc alloy electrodeposits are given in figures 2(a)–(g).

Corrosion potentials of the deposits obtained from baths containing aldehydes offered active values compared to deposit A (table 4). The order of current density is B > C > D > F > E.

3.3c *Impedance diagrams:* Impedance diagrams obtained for various alloy electrodeposits are shown in figures 3(a)–(g). In most of the cases, the impedance diagrams exhibited two semi circles followed by a near linear segment at low frequency end. The appearance of two semi-circles corre-

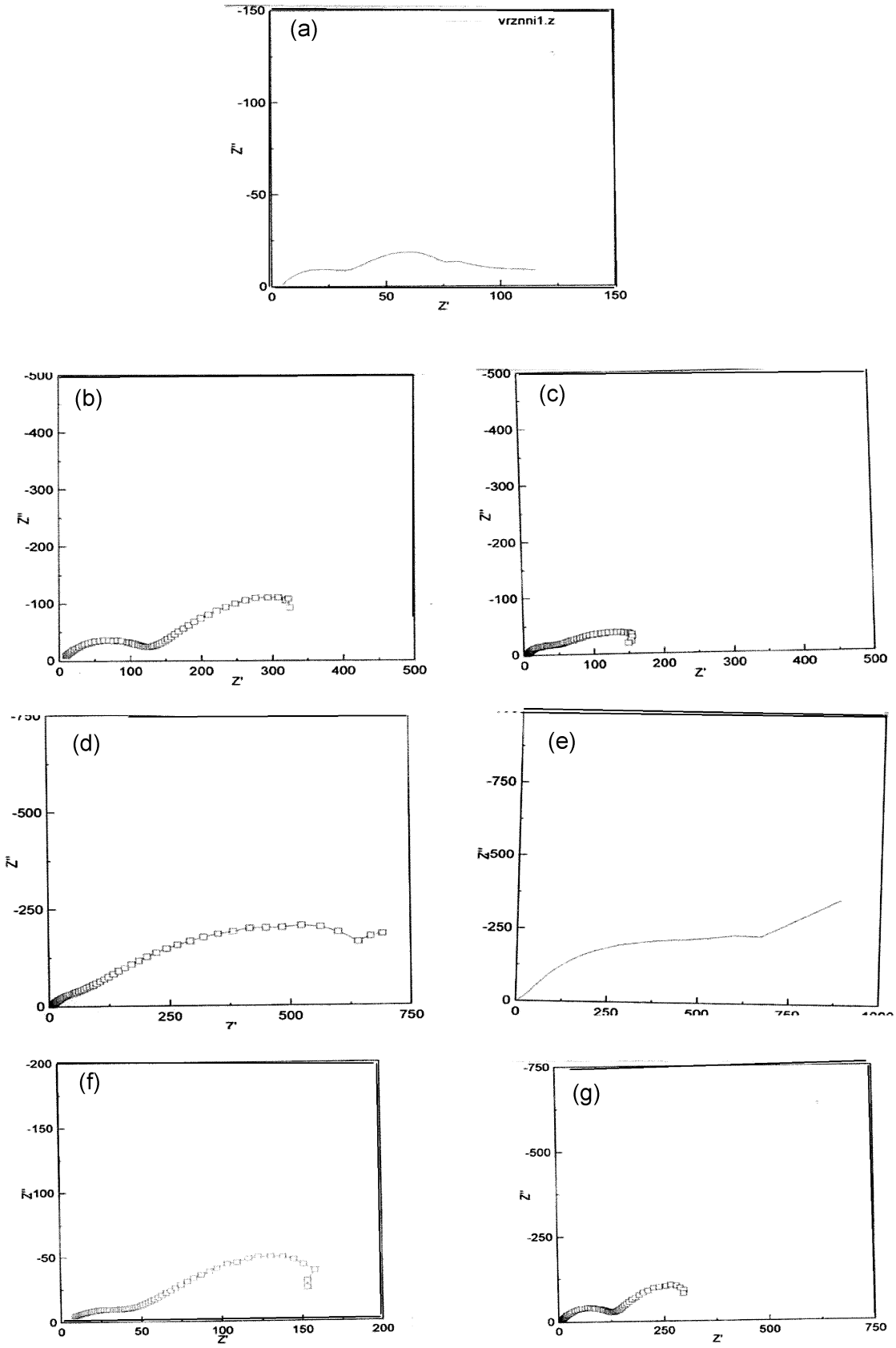

Figure 3. Impedance diagrams for the corrosion in 5% NaCl solution: (**a**) deposit A, (**b**) deposit B, (**c**) deposit C, (**d**) deposit D, (**e**) deposit E, (**f**) deposit F and (**g**) deposit G.

sponds to the presence of two R_c equivalent circuits. The charge transfer resistances and capacitance of the double layer values at the frequency maximum was calculated (table 5). The charge transfer resistances of the second semicircle increased in the deposits obtained from baths containing aldehydes while the double layer capacitances decreased.

3.4 *X-ray diffraction*

Substituted aldehydes like acetaldehyde, anisaldehyde, benzaldehyde, formaldehyde and furfuraldehyde were added individually to zinc alloy plating baths (table 1). On examining the surface, the composition analysis revealed that the aldehydes decreased the zinc content on the surface and anisaldehyde addition brought it to 71·79 (table 2). X-ray diffraction patterns of the electrodeposits revealed (table 6) that reflections were obtained from (330, 411) planes of *d*-Ni_3Zn_{22} phase along with (204) of zinc and (311) of nickel plane. On a few deposits, signals corresponding to (002, 311) of $Zn(OH)_2$ were also seen. In general, addition of substituted aldehydes did not alter the phases present in the alloy (figures 4(a)–(g)).

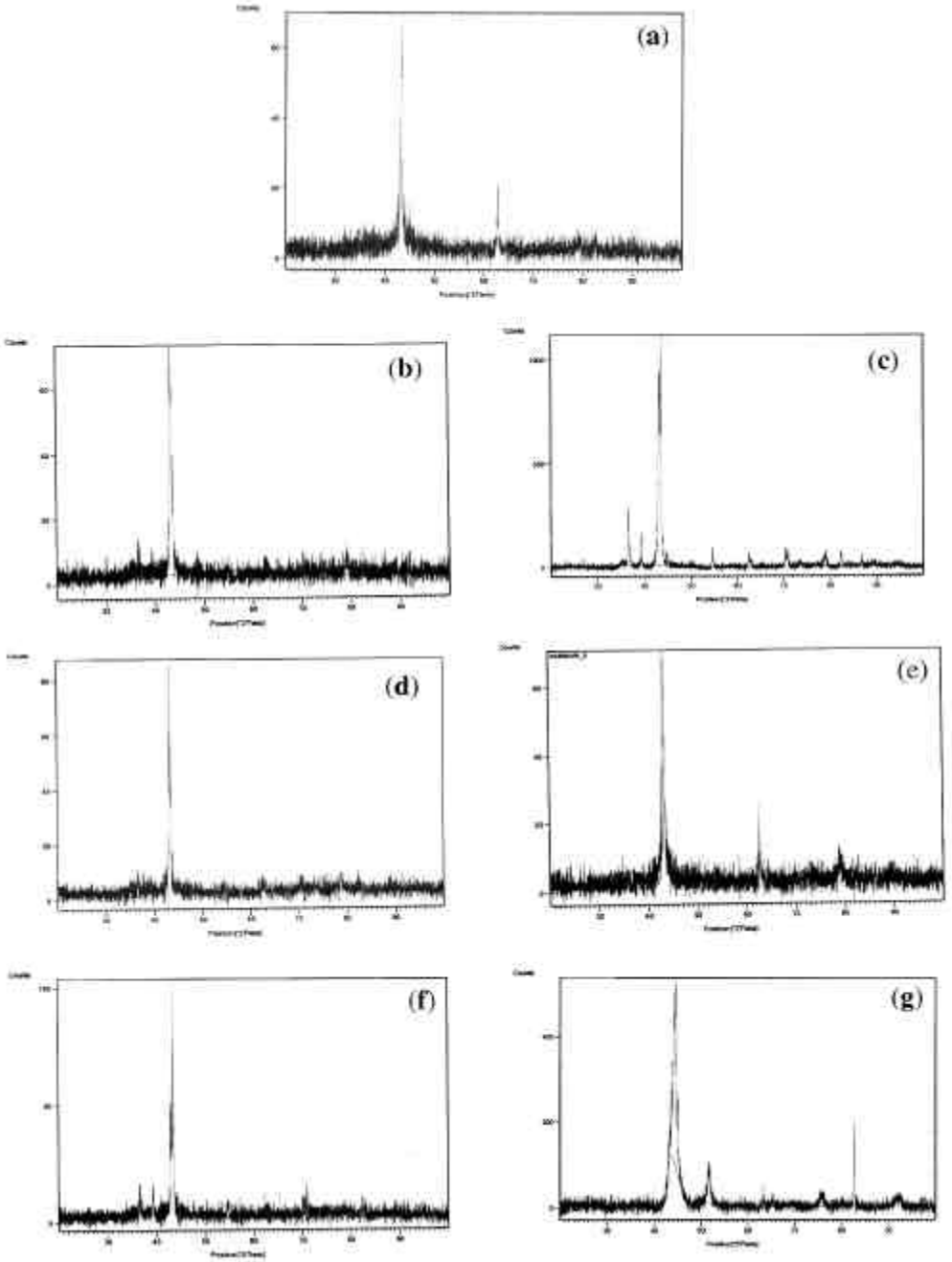

Figure 4. X-ray diffractograms: (**a**) deposit A, (**b**) deposit B, (**c**) deposit C, (**d**) deposit D, (**e**) deposit E, (**f**) deposit F and (**g**) deposit G.

Table 6. Parameters derived from XRD data.

Deposit	2*q*	Average crystal size ( )	'*d*' spacing		*hkl*
			Observed	Standard	
A	43·2551	7·30	2·0896	2·091	330, 411 (Ni_3 Zn_{22}) 101 (Zn)
	92·6388	6·05	1·0651	1·062	311 (Ni)
	35·0	6·0	1·5	1·55	$Zn(OH)_2$ (002, 311)
B	43·2983	5·99	2·0879	2·091	330, 411 (Ni_3 Zn_{22}) 204 (Zn)
	79·0304	2·71	1·2306	1·246	220 (Ni)
C	43·316	1·79	2·0871	2·091	330, 411 (Ni_3 Zn_{22}) 204 (Zn)
	39·2995		2·2002	2·2707	100 (Ni)
D	43·1755	5·99	2·0980	2·091	330, 411, 204 (Zn)
	48·7859	4·32	1·2380	1·246	220 (Ni)
	35·0	6·0	1·45	1·55	$Zn(OH)_2$ (002, 311)
E	43·2343	3·59	2·0909	2·091	330, 411, 204 (Zn)
	78·9364	2·16	1·2384	1·246	220 (Ni)
F	43·0920	5·47	2·0090	2·091	330, 411, 204 (Zn)
	79·5562	4·38	1·2464	1·246	220 (Ni)
G	43·1920	7·30	2·0920	2·091	330, 411, 204 (Zn)
	78·8497	1·65	1·2380	1·246	220 (Ni)
	35·0	6·0	1·45	1·55	$Zn(OH)_2$ (002, 311)

4. Discussion

Organic compounds are added to plating baths to increase polarization even at relatively low current densities. They improve the quality of the deposit in terms of adherence, size and grain homogenization. They may also inhibit the formation of dendrites and whiskers (Meibuhr *et al* 1963). These compounds adsorb on the electrode surface and then block the high energy sites for the crystallization of the metal (Kardos and Foulke 1962). The formation of critical micelle concentration is viewed as a mechanism of the action of organic compounds on the electrodeposition of metals (Aragon *et al* 1992).

In the case of zinc dissolution and deposition (loc.cit), substituted aldehydes adsorb on the surface. The adsorption followed Langmuir adsorption isotherm. This is due to the interaction of lone pair of electrons on the oxygen atom of the molecules with the growing zinc nuclei. The extent of adsorption depends on the electron density of the oxygen atom. The electrodeposition of Zn–Ni alloy is classified as anomalous (Brenner 1963). The deposition of the more noble metal nickel, is suppressed by the preferential deposition of zinc (table 2). For the anomalous codeposition an idea based on the work function was suggested. If the work function of the alloy has been between that of the parent metals then continuous underpotential deposition of the nickel is possible. As the electrodeposition is carried out over a prolonged period it may cause pH to change near the surface. This would result in the precipitation of $Zn(OH)_2$. The anomalous codeposition of Zn–Ni alloy may be due to (i) an increase of the surface pH causing the formation of $Zn(OH)_2$ which may suppress nickel discharge, (ii) zinc deposition may be controlled by mass transport and nickel deposition by kinetics, (iii) the rate of charge transfer of $ZnOH^+$ and $NiOH^+$ species may be responsible and (iv) the monolayer coverage of nickel may be followed by water molecule chemisorption with the formation of $NiOH^+_{ads}$.

As a result of the competition of Zn and Ni ions to occupy active sites, the preferential deposition of zinc and suppression of nickel takes place. As the electrodeposition was carried out for a prolonged period, an increase of surface OH^- ion concentration caused the precipitation of $Zn(OH)_2$. Substituted aldehydes may adsorb on the $Zn(OH)_2$ precipitated layer and prevent the growth of $Zn(OH)_2$. The suppression of $Zn(OH)_2$ growth favoured the discharge of nickel ions. Hence an increased amount of nickel was seen in the surface of alloy deposits B, C, D, E, F and G. The formation of sulphamate bath, *d*-Zn_3Ni_{22}, was favoured as the $Zn(OH)_2$ precipitation was hindered (table 2). The corrosion resistance property of these deposits may be understood from the impedance diagrams. Stern-Geary (1957) showed that the

$$R_{ct} = \text{charge transfer resistance} = \frac{b_a \times b_c}{2 \cdot 303(b_a + b_c) i_{corr}},$$

where i_{corr} is corrosion current density. An increase of R_{ct} corresponds to a decrease in corrosion rate. The appearance of the two semi circles in the impedance diagrams corresponds to the existence of steel/zinc alloy interface and alloy/solution interface. The corrosion behaviour of the coating is decided by the incorporation of aldehydes inside the deposit. The aldehydes inhibit corrosion of the alloy. The charge transfer resistances increased for the second semicircle. These suggest that the aldehydes inclusion decreased the corrosion. The adsorption of the aldehydes and inclusion of them was revealed by the decrease in C_{dl} of the semi circle.

5. Conclusions

The effect of substituted aldehydes on the corrosion behaviour of Zn–Ni alloy electrodeposition from sulphamate bath was studied. The uniform nature of the coatings was observed from microstructure analysis by optical microscopy. The presence of aldehydes in the bath offered deposits with smooth uniform and non porous surfaces. Small spherical crystallites were seen covering the surface. Aldehydes decreased the zinc content on the surface and the addition of anisaldehdye brought it down to 71·7% from 85% in the Zn–Ni alloy deposit obtained from the bath not containing any aldehyde. X-ray patterns of the electro deposit revealed that reflections were obtained from (330, 411) planes of *d*-Ni_3Zn_{22} plane along with (204) of zinc and (311) of nickel planes. Salt spray revealed that except for deposit C, all other deposits postponed white and red rust formation. The positive shift in E_{corr} and decrease in I_{corr} values for the Zn–Ni electrodeposits showed its improved corrosion resistance nature. Adsorption of these aldehydes and their inclusion caused a reduction in corrosion rates.

References

Aragon A, Figuerroa M G F and Gand R E 1992 *J. Appl. Electrochem.* **22** 558

Brenner A 1963 *Electrodeposition of alloys, principles and practice* (NY: Academic Press)

Kardos D and Foulke D G 1962 *Advances in Electrochemistry and Electrochem. Engg* **2** 145

Meibuhr S, Yeager E, Kosawa A and Hororka F 1963 *J. Electrochem. Soc*. **110** 190

Rajagopalan S R 1972 *Metal Finishing* **70** 52

Ravindran Visalakshi and Muralidharan V S 1996 *Indian J. Chem. Technol*. **3** 231

Ravindran Visalakshi and Muralidharan V S 2003 *J. Sci. Ind. Res*. **62** 718

Ravindran Visalakshi, Krishnan R M and Muralidharan V S 1995 *Trans. Inst. Met. Fin.* **43** 189

Shabana Begum S, Muralidharan V S and Mayanna S M 2001 *Portugaliae Electrochem. Acta* **19** 121

Stern M and Geary A L 1957 *J. Electrochem. Soc.* **104** 56

Wagner C and Traud W 1938 *Z. Phys. Chem*. 411

Tsuda T and Kurimoto T 1981 US pat. 4249999